Density-dependent instabilities in correlated two dimensional electron systems

2004 J. Phys.: Condens. Matter 16 3623

(http://iopscience.iop.org/0953-8984/16/21/011)

INSTITUTE OF PHYSICS PUBLISHING JOURNAL OF PHYSICS: CONDENSED MATTER

J. Phys.: Condens. Matter **16** (2004) 3623–3631 PII: S0953-8984(04)70160-5

Density-dependent instabilities in correlated two dimensional electron systems

Arindam Ghosh, Michael Pepper, Harvey E Beere and David A Ritchie

Cavendish Laboratory, University of Cambridge, Madingley Road, Cambridge CB3 0HE, UK

Received 9 October 2003
Published 14 May 2004
Online at stacks.iop.org/JPhysCM/16/3623
DOI: 10.1088/0953-8984/16/21/011

Abstract

We have investigated the electrical transport in mesoscopic low-density 2D electron systems as a function of background disorder. At zero magnetic field, over a specific window of disorder and electron density, an unusual density-dependent oscillatory pattern in conductance was observed as the Fermi energy was swept in the localized regime. The temperature, source–drain bias and magnetic field dependence of transport indicate the formation of a pinned electron solid, which undergoes a series of order–disorder transitions as the electron density is changed by a gate.

In a strongly disordered localized 2D electron system (2DES), experimental [1] and theoretical [2, 4] study of electrical transport at mesoscopic length scales has been extensive. We now know that transport in this regime is dominated by resonant (or elastic) tunnelling (RT), hopping via a small number of isolated impurity states, or the Coulomb blockade (CB) effect in small puddles of electrons, capacitively coupled to the leads. When the amplitude of the background potential fluctuations is reduced, localization occurs at smaller Fermi energy (E_F), and hence at stronger effective Coulomb interaction (U_C) with $U_C/E_F \sim 1/\sqrt{n_s} \gg 1$, where n_s is the electron density. Transport experiments in low-density 2DESs reveal various many-body body phenomena ranging from glassy freezing [5] to electron-assisted hopping [6], but the nature of the ground state, in particular at the mesoscopic scale, is still not well understood. Theoretically, while several forms of charge-density-wave (CDW) ground states have been predicted [7, 8], it is generally agreed that over a specific disorder window the interaction effects would be significantly amplified, leading to modification in the single-particle transport. Here, we have investigated the disorder-enhanced interaction effect in dilute 2DESs as a function of the magnitude of background potential fluctuations. At the mesoscopic length scales, we identify a non-monotonic conductance (G) structure as a function of E_F that could not be associated to conventional RT or CB, but appears to be due to a many-body phase in the correlated regime.

We have used 2DESs formed at high quality modulation-doped GaAs/$Al_xGa_{1-x}As$ heterostructures, where the magnitude and length scale of disorder can be tuned by varying

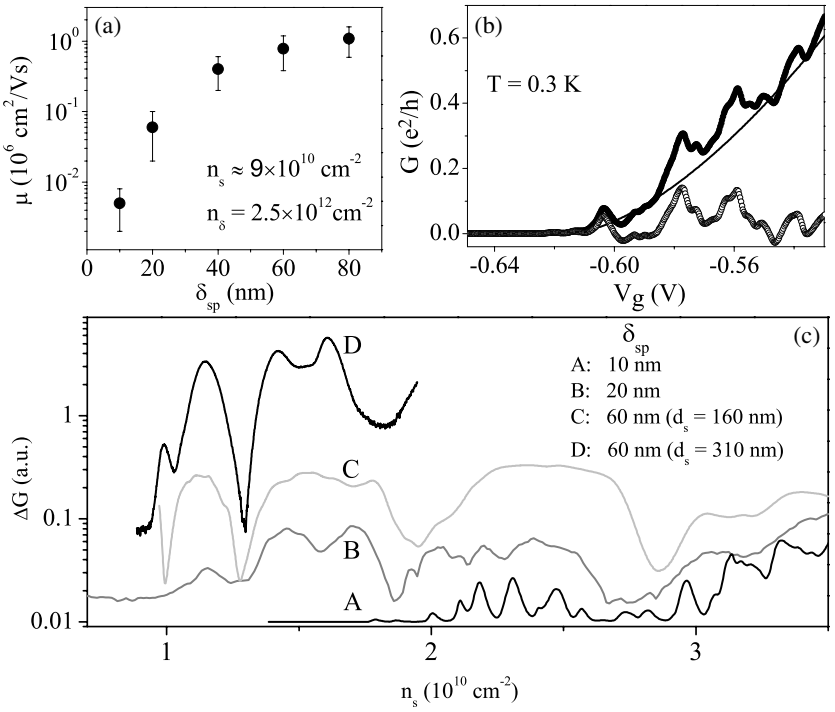

Figure 1. (a) Dependence of the overall mobility μ on the spacer thickness $\delta_{\rm sp}$. The mobility is calculated at electron density $n_{\rm s} = 9 \times 10^{10}$ cm^{-2}. (b) A typical $V_{\rm g}$-dependence of conductance G for a sample with $\delta_{\rm sp} = 60$ nm. The solid curve indicates a smoothly increasing background. The open circles indicate the background-subtracted oscillations (ΔG). (c) Dependence of ΔG on $n_{\rm s}$ in four samples ($n_\delta = 2.5 \times 10^{10}$ cm^{-2}) with varying disorder. The samples are 2 μm $\times$ 2 μm squares. All the traces are obtained at 0.3 K and zero magnetic field. The traces are scaled and vertically shifted for clarity.

the distance ($\delta_{\rm sp}$) and density (n_δ) of the Si-dopants in the δ-doped layer from the 2DES. We have studied a large number of 2DESs with $\delta_{\rm sp}$ ranging from 0 to 80 nm, and n_δ from 2.5 to 10 $\times$ 10^{12} cm^{-2}. In most samples, measurement of the transport and quantum lifetime suggest that the mobility μ in the metallic regime is limited primarily by small-angle scattering. Hence, as shown in figure 1(a), at a given $n_{\rm s}$ ($\approx$9 $\times$ 10^{10} cm^{-2}), the average μ rises by $\sim$3 orders of magnitude when $\delta_{\rm sp}$ is increased from 0 to 80 nm. The electron density $n_{\rm s}$ was varied continuously by a metallic surface gate at a distance $d_{\rm s}$ above the 2DES, $d_{\rm s}$ ranging over 120–330 nm. The sample dimensions were chosen to be in the mesoscopic regime with the length (l) and width (w) varying from 0.4 to 5 μm and 1.5 to 5 μm, respectively. In most samples at $T \approx 300$ mK, freezing of the carriers occurred around $V_{\rm g} \sim -0.3$ to -1.0 V, where $V_{\rm g}$ is the voltage at the surface gate. The electron density achieved at this 'pinch-off' depends on the $\delta_{\rm sp}$, and in cleaner samples (e.g. $\delta_{\rm sp} \sim$ 40–60 nm) $n_{\rm s}$ as low as $\sim$8–10 $\times$ 10^9 cm^{-2} ($U_{\rm C}/E_{\rm F} \sim 6$) could be achieved. The conductance G was measured by the standard low-frequency two or four probe method with a measuring bias $V_{\rm sd} \ll k_{\rm B}T/e$. When $G \ll e^2/h$, the temperature dependence of G was found to obey the variable-range hopping law, $G(T) \sim G_0 \exp[-(T_0/T)^p]$, where T_0 is the density-dependent activation energy scale and $p \sim 0.3$–0.5. In about 10–15% of the relatively disordered samples (mostly with $\delta_{\rm sp} \lesssim$ 15–20 nm) at low densities, we found a slow drift in G over a large timescale $\tau \sim$ 10–1000 s,

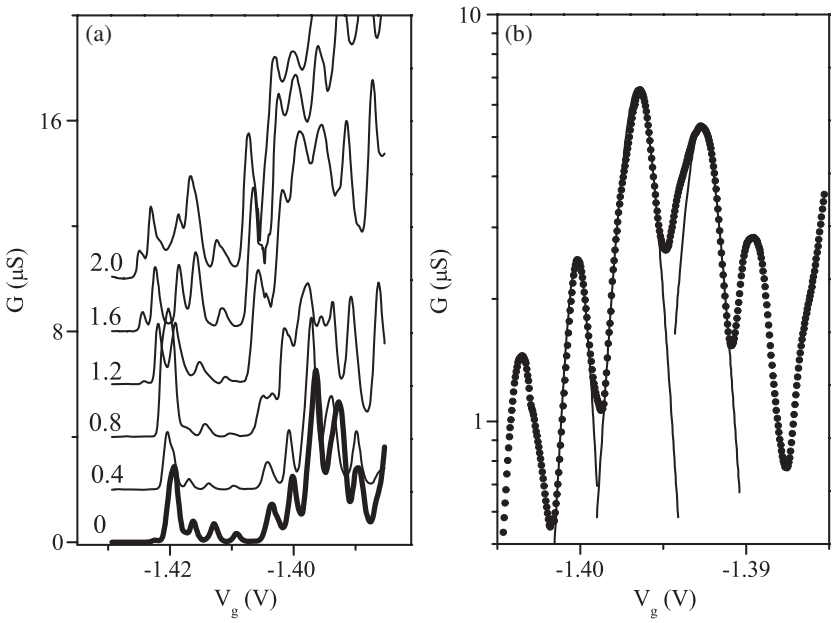

Figure 2. Coulomb blockade oscillations in a disordered sample with $\delta_{sp} = 10$ nm. The data was recorded at $T \approx 0.3$ K. (a) Traces at different source–drain fields. The numbers indicate the source–drain bias in millivolts. The thick solid curve identifies the zero-bias trace. Successive traces are shifted vertically by 2 μS for clarity. (b) Line-shape of the individual peaks. The solid curve denote a thermally broadened $\cosh^{-2}(x)$ line-shape.

reminiscent of a glassy behaviour [5]. Our analysis was, however, based on the samples which were extremely stable, and did not show any drift within the experimental accuracy (better than 0.1%) at any value if n_s. Due to the uncertainty in measuring the exact geometry of the active region, primarily due to the lateral depletion at the mesa-walls, we have reported the data in terms of conductance G, rather than the conductivity σ. Since most of the discussions are based only on relative changes in G, this does not affect the main conclusion of the paper.

In figure 1(b), the solid circles illustrate a typical G–V_g trace at $B = 0$, obtained from a 2 μm $\times$ 2 μm sample with $\delta_{sp} = 60$ nm moderately disordered with a high dopant density ($n_\delta = 10^{13}$ cm^{-2}). In the localized regime ($V_g \lesssim -0.5$ V) G displays a non-monotonic structure as the Fermi energy is swept across the band tail. The oscillations are highly reproducible and, when the smoothly increasing background (solid curve) is subtracted, these appear as a superposition of small-amplitude, rapid fluctuations on a large-amplitude slowly varying component. In figure 1(c), we show the behaviour of these two components when δ_{sp}, i.e. the effective disorder, is varied. When disorder is strong, as in sample A with $\delta_{sp} = 10$ nm, the rapid fluctuations become sharply peaked and quasi-periodic in V_g.

In order to determine the origin of these rapid component, we have studied its dependence on the Fermi energy and source–drain field in several samples fabricated from the wafer with $\delta_{sp} = 10$ nm. Figure 2 illustrates this with a typical 2 μm $\times$ 2 μm sample measured at $T \approx 0.3$ K. The modulation in the zero-bias conductance is clearly observable (figure 2(a)), which gets obscured by the appearance of new sharp peaks as the source–drain bias was increased. This is a clear signature of the Coulomb blockade (CB) effect, where new peaks arise with the inclusion of additional single-particle states between the chemical potentials of the source and drain [3]. The conductance around these peaks was found to vary as

$\sim \cosh^{-2}(\beta \Delta V_g)$, where β is a numerical constant depending on the temperature and the compressibility of the system [4]. As shown in figure 2(b), this line-shape provides further evidence of thermally broadened tunnelling through nearly isolated puddles of electrons. Formation of such puddles are expected in a strongly disordered 2D mesoscopic system [4]. Typical charging energy, e^2/C_Σ, where C_Σ is the total capacitance of the conductance-limiting puddle, was found to lie within ~0.5–1.5 meV. From $C_\Sigma \approx 4\epsilon_0\epsilon_r d_p$, we find, $d_p \sim 0.2$–$0.4\ \mu$m, where d_p is the diameter of the puddle. Note that $d_p \gg 1/\sqrt{n_\delta}, \delta_{sp}$, which implies a spatial correlation in the δ-doped layer. As the amplitude of potential fluctuations is reduced by increasing δ_{sp}, for example, from sample B with $\delta_{sp} = 20$ nm to sample C with $\delta_{sp} = 60$ nm, the relative amplitude of the CB oscillations is suppressed, and the slow background oscillations dominate the non-monotonicity of conductance in the clean samples up to δ_{sp} as large as 80 nm.

While the amplitude of the oscillations depends strongly on the local disorder, hence vary from sample to sample even for a given δ_{sp}, an intriguing feature of traces shown in figure 1(c) is the overall similarity in the positions of the conductance minima of the slow oscillations, when expressed in terms of n_s. We have used a linear calibration of n_s with V_g as $n_s = C_s(V_g - V_{gp})$, obtained from the quantum Hall measurements in the metallic regime ($C_s \approx \epsilon/ed_s$, is the specific capacitance, and V_{gp} is the pinch-off voltage). These density-dependent oscillations (DDOs) are clearly distinct from CB oscillations, which are periodic in V_g. To investigate this, we have varied C_s over a factor of ~2–3, and observed the width of the DDOs in V_g to change accordingly. In figure 1(c), in spite of the specific capacitance of sample D being roughly one-third that of sample B ($C_s^D/C_s^B \approx 0.37$), the strong minima appear at similar values of n_s. Typically, 2–4 periods of DDOs are observed in most localized samples with large δ_{sp}. We have restricted the analysis within the strongly localized regime since,

(1) when $G \gtrsim e^2/h$, interference effects like universal conductance fluctuations lead to additional structures in G obscuring the DDOs, and
(2) at higher V_g, the dependence of n_s on V_g deviates from linearity, introducing a systematic error in the positions of the minima.

Denoting n_s at the minima as n_{min}, we have compiled the n_{min}-values from 22 samples with varying size and δ_{sp} (figure 3). In order to minimize the effect of CB oscillations, we have only considered samples with $\delta_{sp} \geqslant 20$ nm. The set of n_{min} from a given sample depends on the range of n_s scanned by V_g, and hence depends on the local disorder. The histogram clearly shows a clustering of n_{min} around a few critical values indicated by the strong peaks. The n_{min}-values originating due to CB forms an uniform background within count range $N_c \lesssim 2$–3. The width of each peak is dominated by the measurement uncertainty of V_{gp} (~10%). Within the experimental accuracy, we found the critical n_{min} to be insensitive to the sample dimensions, however the magnitude of the oscillations becomes too small to observe beyond the scale of $\gtrsim 20\ \mu\text{m} \times 20\ \mu\text{m}$.

In order to understand the DDOs, we now focus on the maxima and minima as the T and source–drain field (V_{sd}) are varied. This is illustrated in figure 4. In figure 4(a), T-dependence of two successive sets of maxima and minima, denoted by 1 and 2, is shown over a range of 0.3–4.5 K. The data was obtained in a $2\ \mu\text{m} \times 2\ \mu\text{m}$ sample with $\delta_{sp} = 20$ nm and $d_s = 120$ nm. Even though the rather large width of the peaks in V_g could be explained in the framework of RT (or CB) by assuming a strong coupling of the localized state to the leads so that the tunnel rate $\Gamma \gg T$, we find such an explanation untenable on the following grounds. The T-dependence of G_{max}/G_{min} shown in figure 4(b) identifies a threshold temperature T_{th} (indicated by the arrows) for both sets, below which the G_{max}/G_{min} is essentially T-independent. For set-2, which is at a higher n_s, we find T_{th} is lower than that of set-1. Since $T_{th} \sim \Gamma$, this implies a

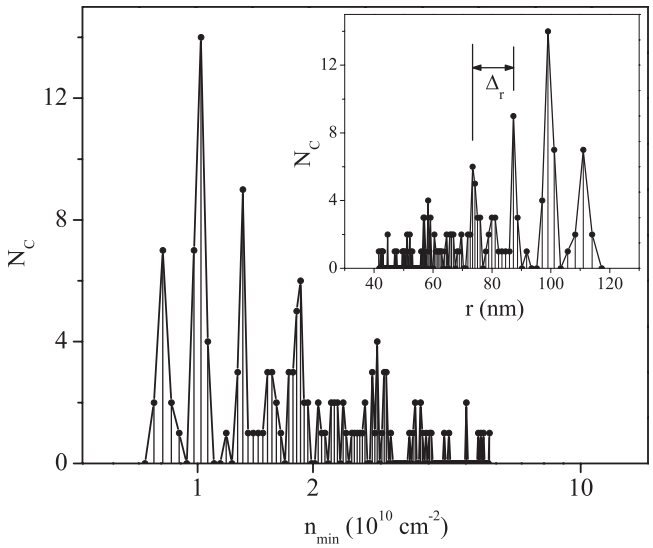

Figure 3. A histogram of electron densities $n_{\rm min}$ at the local conductance minima in 22 samples. $N_{\rm c}$ denotes the count in a given window of density. The samples were fabricated from wafers with dopant densities ranging from $n_\delta = 2.5$–10×10^{12} cm^{-2} in the δ-doped layer. Inset: same histogram plotted as a function of the electron separation $r = 1/\sqrt{n_{\rm min}}$. $\Delta_{\rm r}$ is the separation of the successive strong peaks in terms of r.

larger tunnel rate at lower $n_{\rm s}$, which is counter-intuitive, since at lower $n_{\rm s}$ screening would be less effective resulting in stronger tunnel barriers.

Figure 4(c)–(e) shows the non-linear characteristics of the DDOs in a 2 μm $\times$ 2 μm sample with $\delta_{\rm sp} = 60$ nm. $V_{\rm g}$-dependence of the linear conductance G is shown in the inset of figure 4(e), where we have identified and numbered every individual maximum (open circles) and minimum (solid circles). The differential conductance $\mathrm{d}I/\mathrm{d}V_{\rm sd}$ at the minima shows a clear gap and threshold-like behaviour in the $V_{\rm sd}$-dependence (figure 4(c)). The gap becomes weaker at higher $n_{\rm s}$. Taking the gap $\sim$0.08 meV at minimum 2, and assuming that it arises from the charging energy e^2/C_Σ of CB, we find the diameter of the conductance limiting dot $d_{\rm dot} > 4$ μm, which is larger than the sample dimension itself. Furthermore, a dot as large as the sample would be purely classical with periodicity $\Delta V_{\rm g} = e/C_{\rm g} \lesssim 0.1$ mV, about two orders of magnitude smaller than the experimentally observed separation between the maxima and minima ($C_{\rm g} \sim \epsilon_0 \epsilon_{\rm r} d_{\rm dot}^2/d_{\rm s}$, is the gate-2DES capacitance).

An important feature of the non-linear transport is the cusp-like sublinear enhancement of $\mathrm{d}I/\mathrm{d}V_{\rm sd}$ in the range $V_{\rm sd} > V_{\rm th}$, where $V_{\rm th}$ is the threshold voltage indicated by the arrows in figure 4(c). In figure 4(e) we have plotted $\mathrm{d}I/\mathrm{d}V_{\rm sd}$ as a function of the reduced source–drain voltage $(V_{\rm sd} - V_{\rm th})/V_{\rm th}$ for the first three minima. We find $\mathrm{d}I/\mathrm{d}V_{\rm sd}$ to behave as a power law with $\mathrm{d}I/\mathrm{d}V_{\rm sd} \sim (V_{\rm sd}/V_{\rm th} - 1)^\zeta$, where $\zeta \approx 0.8$, over about one order of magnitude of $V_{\rm sd}$, equivalent to $\sim$2 orders of magnitude of I. At higher $V_{\rm sd}$, $\mathrm{d}I/\mathrm{d}V_{\rm sd}$ becomes slower as I asymptotically approaches the linear regime.

The threshold behaviour of $\mathrm{d}I/\mathrm{d}V_{\rm sd}$ at the local conductance minima resembles sliding transport of a pinned charge-density wave above the depinning threshold [9, 10]. In this context, the exponent $\zeta \approx 0.8$ shows remarkable agreement to that in the collective flow of charge in 2D array of metallic dots [9] or in the plastic flow of a weakly disordered Wigner solid [11]. Theoretically [12], $\zeta = 2/3$ is obtained when the 2D system is spatially ordered. Hence

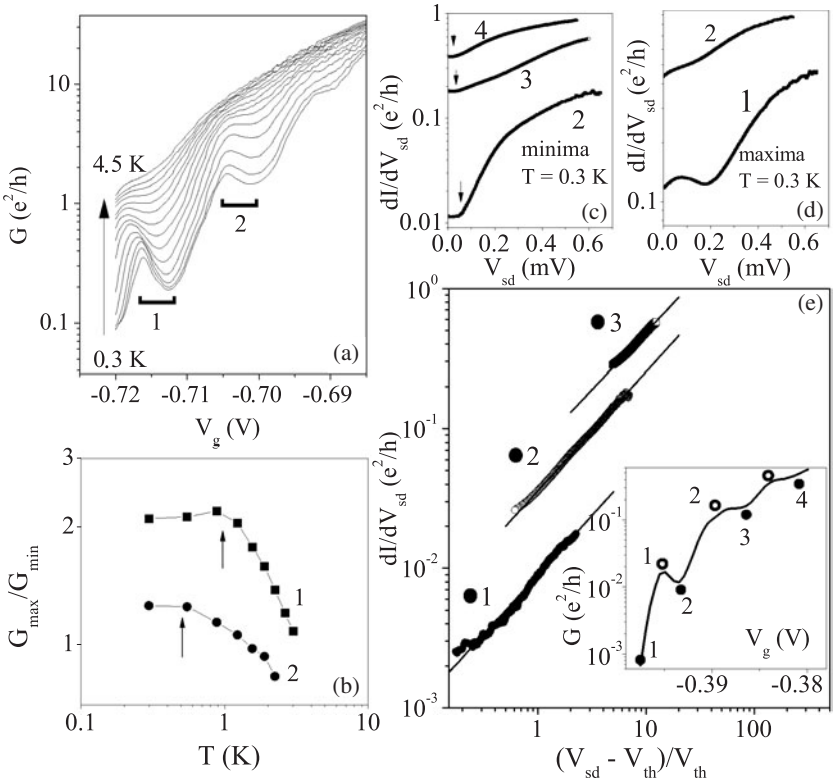

Figure 4. The temperature T and source–drain field $V_{\rm sd}$ dependence of the density-dependent oscillations: (a) T dependence from 0.3 to 4.5 K. Two sets of successive maxima and minima are denoted by 1 and 2. The data was obtained in a sample with $\delta_{\rm sp} = 20$ nm and $n_\delta = 2.5 \times 10^{12}$ cm^{-2}. (b) T-dependence of the ratio of $G_{\rm max}$ and $G_{\rm min}$ for set-1 and set-2. The temperature threshold ($T_{\rm th}$) is indicated by arrows. (c), (d) $V_{\rm sd}$ dependence of the differential conductance $\mathrm{d}I/\mathrm{d}V_{\rm sd}$ at the minima and maxima, respectively. Arrows indicate the threshold voltage at the minima. The data was obtained in a sample with $\delta_{\rm sp} = 60$ nm at $T = 0.3$ K. (e) $\mathrm{d}I/\mathrm{d}V_{\rm sd}$ as a function of the reduced voltage $(V_{\rm sd} - V_{\rm th})/V_{\rm th}$ at three of the minima. Note the power law rise in $\mathrm{d}I/\mathrm{d}V_{\rm sd}$. The solid lines indicate a slope of ≈0.8. Inset: conductance in log-scale at zero source–drain bias. The solid and open markers indicate the positions of the minima and maxima, respectively, for which the differential conductance has been shown.

the DDOs appear to be associated to a CDW ground state of the 2DES, where the electrons are distributed in a rigid crystalline array. Microwave resonance studies have indicated such a crystalline order in high-mobility 2DESs at a very similar range of $n_{\rm s}$ [13]. Even though the range of $n_{\rm s}$ is too large for a conventional Wigner crystallization, numerical studies show that in the presence of weak pinning the crystallization can be stabilized at effective Coulomb interaction as low as $U_{\rm C}/E_{\rm F} \sim 7.5$ [7]. Indeed, in a recent magneto-transport study we have obtained clear evidence of a rigid self-localized electron phase in similar mesoscopic systems [14].

In a pinned electron solid, any characteristic length scale in the background potential may give rise to a commensurability oscillation in the pinning potential [15]. To investigate the possibility of such an effect we have analysed the histogram of $n_{\rm min}$ values in terms of the mean electron separation $r = 1/\sqrt{n_{\rm min}}$. This is shown in the inset of figure 3. Note that the peak separation is relatively more uniform with the separation between the strong peaks being

$\Delta_r \approx 11 \pm 2$ nm. At higher n_s, the peak separation appears to have increased slightly, which can be attributed to the sublinearity of the n_s–V_g relation at high n_s. Assuming the dopant distribution to provide the external length scale, we have varied the dopant concentration n_δ by a factor of ≈4 from $n_\delta = 2.5 \times 10^{12}$ cm^{-2} ($d_\delta = 1/\sqrt{n_\delta} \approx 6$ nm) to $n_\delta = 1 \times 10^{13}$ cm^{-2} ($d_\delta \approx 3$ nm). Within the experimental accuracy, however, we have not observed any significant reduction in Δ_r. Even though this could be due to a higher compensation factor at high dopants densities, we also note that in most cases the spacer width δ_{sp} is $\gg d_\delta$, and the granularity in the background potential due to individual donors should be exponentially suppressed.

Since the commensurability effect only modulates the pinning potential, it cannot explain the peak in dI/dV_{sd} at non-zero V_{sd} at the conductance maxima (figure 4(d)). The amplitude of the DDOs is essentially determined by the position and width of this peak, which depend on local disorder and thermal history of the sample. The position of the peak was found within the range ∼0.02–0.1 mV in all the samples. Note that, for RT (or CB), this peak is expected at $V_{sd} = 0$. These observations lead to the following possible mechanism for DDOs. In a pinned electron solid, when the electron number is changed using the gate, an 'impurity band' of interstitials (or vacancies) may form as a complete reorganization of the solid may be energetically unfavourable [7, 16]. Apart from enhancing the screening of the pinning potential, this would also raise the energy of the system through strain and strong zero-point fluctuations, towards a solid-to-fluid transition. However, close to the fluid state the energy cost of a collective reorganization is much less, and the system may re-condense in a solid with different lattice parameters. A quantitative analysis leading to the observed $\Delta_r \approx 11$ nm is beyond the scope of this paper. However, the similarity of Δ_r to the effective Bohr radius a_B^* (≈10.5 nm) in GaAs systems was noted in early experiments, where the DDO was attributed to a fundamental instability of the pinned 2DES to electron–electron interaction [17].

We investigated the possibility of such an order–disorder transition by studying the low-field magneto-conductance (MC) in perpendicular magnetic field B. Figure 5(a) illustrates the MC at the adjacent maximum and minimum (indicated by the arrows) obtained in a 2 μm × 2 μm 2DES with a 60 nm spacer. At $B \gtrsim 0.5$–1 T, MC decreases rapidly according to $G(B) \sim \exp(-\alpha B^2)$, at all V_g in the localized regime, indicating the compression of the electron wavefunction around isolated impurity states [18]. At low B MC showed qualitatively different behaviour at the maximum and minimum of the DDOs. At the minimum, a strong positive MC (PMC) (∼20%) was observed at very low fields ($B \lesssim 0.2$ T), while at the maximum, both the magnitude and the characteristic field-scale (B_c) of the PMC were reduced[1]. Obtaining B_c roughly from the field at which PMC is maximum, we have shown the dependence of B_c on V_g in figure 5(b). The non-monotonic behaviour of B_c clearly excludes the mechanism of delocalization to the quantum Hall state in our samples at the filling factor $\nu = 2$ [19]. Hence the most likely origin of the PMC is an interference effect, for example, the 'forward interference' in the strongly localized regime, where the intermediate destructive interferences of the hopping electrons are suppressed by the magnetic field [20]. In such a case, B_c depends on the localization radius ξ of the electrons as $B_c \sim h/e\xi^2\alpha(T)$, where $\alpha(T) \sim (T_0/T)^{3p/2}$ is a T-dependent hopping parameter. In figure 5(b), delocalization of the electrons is evident at the conductance maximum, where ξ shows an increase by several factors. However, even though qualitatively the same behaviour is observed in all samples, the increase in ξ depends on local disorder. As shown in figure 5(c), the relative change in B_c at the maxima are strongly reduced when the local disorder is enhanced in a sample with a smaller spacer ($\delta_{sp} = 40$ nm). Around a minimum, B_c is nearly constant, and since α varies roughly over ∼1–5 at $T \approx 0.3$ K

[1] For $B \gtrsim 0.1$–0.15 T there is weak oscillatory pattern superimposed on the magneto-conductance traces. This arises from the Subnikov–de Haas oscillations of the ungated part of the 2DES. The relative magnitude of this component decreases as the sample becomes more insulating.

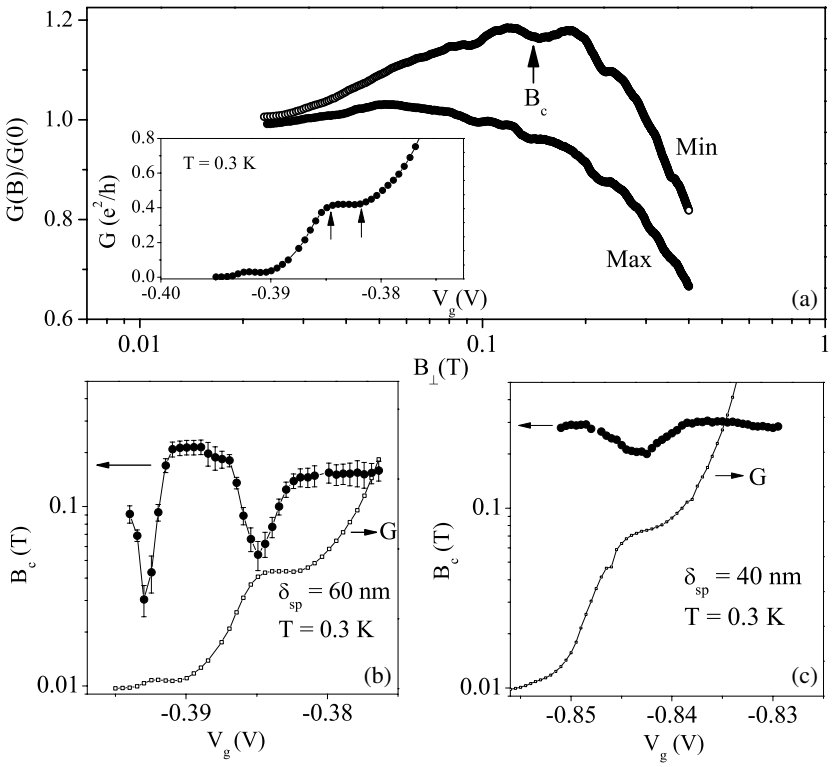

Figure 5. (a) Perpendicular magnetic field dependence of G at a local maximum and minimum, obtained in a sample with $\delta_{sp} = 60$ nm (dimension: 2 μm $\times$ 2 μm). The inset shows a $B = 0$ conductance trace as a function of V_g. (b) Variation of the characteristic field B_c as a function of V_g. The $B = 0$ conductance is also shown for comparison. (c) V_g-dependence of B_c of a relatively disordered sample ($\delta_{sp} = 40$ nm). Even though the qualitative behaviour is similar, the relative change in B_c is suppressed.

($T_0 \sim$ 1–10 K and $p \sim$ 0.3–0.5, from T-dependence of linear conductance), the absolute magnitude of ξ at the minima was found to lie between $\sim$70 and 130 nm, which is close to the separation among the electrons themselves. A more quantitative analysis would require a better estimate of B_c from an analytical description of the B-dependence of MC.

In summary, we have experimentally observed a density-dependent conductance oscillations in low-density mesoscopic 2DESs, that cannot be described by the resonant tunnelling or Coulomb charging effects. In source–drain field, the behaviour of conductance agrees with that of a sliding CDW, implying the ground state of the system to be a pinned electron solid. In this context, the conductance oscillations appear to be due to an energy instability in the solid to the formation of defects, leading to a series of order–disorder transitions. The low-field magneto-conductance in perpendicular magnetic field also indicates an enhancement of the electron localization length at the conductance maxima, supporting this picture.

Acknowledgments

We acknowledge several fruitful discussions with Dr Chris Ford, Dr Ben Simons, Dr Nigel Cooper and Professor A Slutskin. We also thank EPSRC for funding the project.

References

[1] Fowler A B, Timp G L, Wainer J J and Webb R A 1986 *Phys. Rev. Lett.* **57** 138
Scott-Thomas J H F *et al* 1989 *Phys. Rev. Lett.* **62** 583
Savchenko A K *et al* 1995 *Phys. Rev.* B **52** R17021
[2] Azbel M Ya and Soven P 1983 *Phys. Rev.* B **27** 831
[3] Kouwenhoven L P *et al* 1997 *Mesoscopic Electron Transport* (*NATO ASI Series E* vol 345) ed L L Sohn, L P Kouwenhoven and G Schön (Dordrecht: Kluwer) pp 105–214
[4] van Houten H, Beenakker C W J and Staring A A M 1991 *Single Charge Tunnelling Coulomb Blockade Phenomena in Nanostructure* (*NATO ASI Series*) pp 167–216
[5] Vaknin A, Ovadyahu Z and Pollak M 1998 *Phys. Rev. Lett.* **81** 669
Bielejec E and Wu W 2001 *Phys. Rev. Lett.* **87** 256601
Bogdanovich S and Popovic D 2002 *Phys. Rev. Lett.* **88** 236401
[6] Gershenson M E, Khavin Yu B, Reuter D, Schafmeister P and Wieck A D 2000 *Phys. Rev. Lett.* **85** 1718
Khondaker S I, Shlimak I S, Nicholls J T, Pepper M and Ritchie D A 1999 *Phys. Rev.* B **59** 4580
[7] Chui S T and Tanatar B 1995 *Phys. Rev. Lett.* **74** 458
[8] Koulakov A A, Fogler M M and Shklovskii B I 1996 *Phys. Rev. Lett.* **76** 499
Slutskin A A, Slavin V V and Kovtun H A 2000 *Phys. Rev.* B **61** 14184
[9] Kurdak C, Rimberg A J, Ho T R and Clarke J 1998 *Phys. Rev.* B **57** R6842
[10] Goldman V J *et al* 1990 *Phys. Rev. Lett.* **65** 2189
[11] Reichhardt C, Olson C J, Grønbech-Jensen N and Nori F 2001 *Phys. Rev. Lett.* **86** 4354
[12] Middleton A A and Wingreen N S 1993 *Phys. Rev. Lett.* **71** 3198
[13] Ye P D *et al* 2002 *Phys. Rev. Lett.* **89** 176802
[14] Ghosh A *et al* 2004 at press
(Ghosh A *et al* 2004 *Preprint* cond-mat/0403560)
[15] Glazman L I, Ruzin I M and Shklovskii B I 1992 *Phys. Rev.* B **45** 8454
[16] Okamoto T and Kawaji S 1998 *Phys. Rev.* B **57** 9097
[17] Pepper M 1979 *J. Phys. C: Solid State Phys.* **12** L617
[18] Ye Q Y, Shklovskii B I, Zrenner A, Koch F and Ploog K 1990 *Phys. Rev.* B **41** 8477
[19] Jiang H W, Johnson C E, Wang K L and Hannahs S T 1993 *Phys. Rev. Lett.* **71** 1439
[20] Nguen V L, Spivak B Z and Shklovskii B I 1985 *Sov. Phys.—JETP* **62** 1021
Schirmacher W 1990 *Phys. Rev.* B **41** 2461